# Survey of EUV Impurity Line Spectra and EUV Bremsstrahlung Continuum in LHD*)

Chunfeng DONG, Shigeru MORITA[1)], Malay Bikas CHOWDHURI[2)] and Motoshi GOTO[1)]

*Department of Fusion Science, Graduate University for Advanced Studies, Toki 509-5292, Gifu, Japan*
[1)]*National Institute for Fusion Science, Toki 509-5292, Gifu, Japan*
[2)]*Institue for Plasma research, Bhat, Gandhinagar 382428, Gujarat, India*

(Received 5 January 2011 / Accepted 14 February 2011)

Radial profiles of impurity spectral line emissions in extreme ultraviolet (EUV) range (60-400 Å) are surveyed for impurity seeded discharges in Large Helical Device (LHD). The line emissions from light impurities such as helium, carbon and neon are located in the edge ergodic layer ($1.0 \leq \rho \leq 1.2$) except for CV and CVI, which are located in region of $0.8 \leq \rho \leq 1$. In contract, the line emissions from heavy impurities such as iron are widely located over the whole plasma region as a function of ionization energy. On the other hand, the radial profile of bremsstrahlung continuum radiation is also clearly recorded in the EUV spectrum observed from high-density discharges with hydrogen pellet injection. Wavelength intervals available for the absolute sensitivity calibration of the present space-resolved EUV spectrometer system are listed with dominant line emissions which are useful as a wavelength marker.



Keywords: EUV spectra, radial profile, light impurity, heavy impurity, bremsstrahlung continuum

DOI: 10.1585/pfr.6.2402078

## 1. Introduction

Spectroscopy plays an essential role in plasma diagnostics of magnetically confined fusion research [1]. In particular, impurity diagnostics is very important in studying energy balance of additionally heated plasmas and achieving high-performance plasmas through confinement improvement. Extreme ultraviolet (EUV) spectrometer is necessary to observe the impurity lines, since the wavelengths emitted from the plasma core become shorter in high-temperature fusion plasmas. Two EUV spectrometers working in wavelength range of 10-130 Å called 'EUV_short' and 50-500 Å called 'EUV_long' have been installed in LHD as impurity monitors after technical developments over several years [2, 3]. EUV spectroscopy combining X-ray and EUV spectrometers which can be operated in wavelength range of 5-500 Å has been also developed in NSTX tokamak to measure both intrinsic light and heavy impurities [4]. However, the EUV spectrometer having spatial resolution has not generally reported until now whereas radial profiles of impurity lines are necessary for analyzing the impurity behavior in detail. Recently, a space-resolved EUV spectrometer working in wavelength range of 60-400 Å has been developed in LHD to measure the radial profile of impurity line emissions for the impurity transport study and the radial profile of bremsstrahlung continuum for absolute sensitivity calibration of the spectrometer and effective ion charge ($Z_{\mathrm{eff}}$) measurement [5].

*author's e-mail: dong.chunfeng@nifs.ac.jp*

*) This article is based on the presentation at the 20th International Toki Conference (ITC20).

In recent two decades, EUV spectra emitted from various kinds of elements have been systematically investigated in fusion devices by means of laser blow-off and impurity pellet injection technique [6,7]. The EUV spectra of highly-ionized strontium and zirconium injected with the laser blow-off technique are identified in wavelength range of 10-330 Å on TFR tokamak [8], and heavy ion spectra from rare gases such as krypton [8] and xenon [9] are studied. EUV spectra are also studied in Alcator C-Mode tokamak for intrinsic carbon and molybdenum impurities [10] and in PLT tokamak for highly-ionized zirconium and molybdenum [11]. In LHD, a double structure impurity pellet [12] with high-$Z$ material of molybdenum and tungsten has been used for the study to avoid the ionization in the ergodic layer. The EUV line emissions are analyzed for both elements [13]. All the analyses are focused on the wavelength identification. Any radial information on such ions has not been yet investigated in the EUV wavelength region. Moreover, in the case of light impurities such as carbon and oxygen several intense line emissions with different principal quantum numbers in the transition exist in the EUV wavelength range. The EUV line emissions from the light impurities are extremely useful to the impurity transport study in the edge ergodic layer. In this paper, the radial profiles of impurities in different charge states are reported with spectral identification. Radial profiles of EUV bremsstrahlung continuum are also presented and available wavelength intervals for the bremsstrahlung continuum measurement are listed for the absolute calibra-

tion of the present space-resolved EUV spectrometer. It is noted here that 'radial profile' expressed in the present paper means the radial profile of chord-integrated line emissions, not the local emissivity profile after Abel inversion.

## 2. Experimental Conditions

The vertical profiles of impurity line emissions are measured by the space-resolved flat-field EUV spectrometer with a varied line spacing holographic grating (1200 grooves/mm at grating center). A good vertical spatial resolution of 15 mm is obtained when a space-resolved slit of 0.5 mm in width is used. Impurity spectral lines are recorded by a back-illuminated chargecoupled device (CCD) detector with a pixel size of $26 \times 26\,\mu m^2$ and pixel numbers of $1024 \times 255$, which can be moved to survey the wavelength range of 60 to 400 Å. Observable wavelength interval, $\lambda_I$, of the EUV spectrometer, which is defined by the CCD size (6.6 mm) along the wavelength dispersion, varies with the wavelength, e.g., $\lambda_I$ = 30 Å at 60 Å and $\lambda_I$ = 65 Å at 400 Å. The spectral resolution $\Delta\lambda$, is really good, e.g., $\Delta\lambda$ = 0.3 Å at 100 Å and $\Delta\lambda$ = 0.5 Å at 400 Å when the entrance slit width is 100 μm. The vertical observation range of the EUV spectrometer perpendicular to the wavelength dispersion is approximately 50 cm and also limited by the CCD size (26.6 mm). A half of the LHD plasma can be then observed at horizontally elongated plasma cross section. It is noted that all the radial profiles presented in this paper are taken at upper half of the LHD plasmas.

The impurities contained in LHD plasmas are always dominated by carbon as the intrinsic impurity released from divertor plates made of carbon. Oxygen is appeared only in the beginning of experimental campaign, if the boronization is not sufficient. Metal impurities such as iron can be also observed as an intrinsic impurity, but the amount is usually very less ($n_{Fe}/n_e < 10^{-4}$). On the other hand, several impurity elements are externally introduced in the LHD plasmas for a variety of experimental purposes. For instance, neon is frequently used to increase electron temperature ($T_e$) and ion temperature ($T_i$) and to cool the edge plasma for production of detached plasmas. Argon is usually used to measure the central ion temperature ($T_i(0)$) from Doppler broadening of He-like ArXVII using crystal spectrometer. Heavy metals like iron are injected by the impurity pellet injector to study the impurity transport and the atomic physics.

## 3. EUV Impurity Line Spectra

### 3.1 Two-dimensional CCD images of line emissions

The vertical profiles of impurity line emissions are shown in Figs. 1 (a)-(i) for different wavelength ranges. The two-dimensional CCD images of spectral lines are exposed from typical hydrogen discharges at the beginning of experimental campaign with relatively high line-averaged

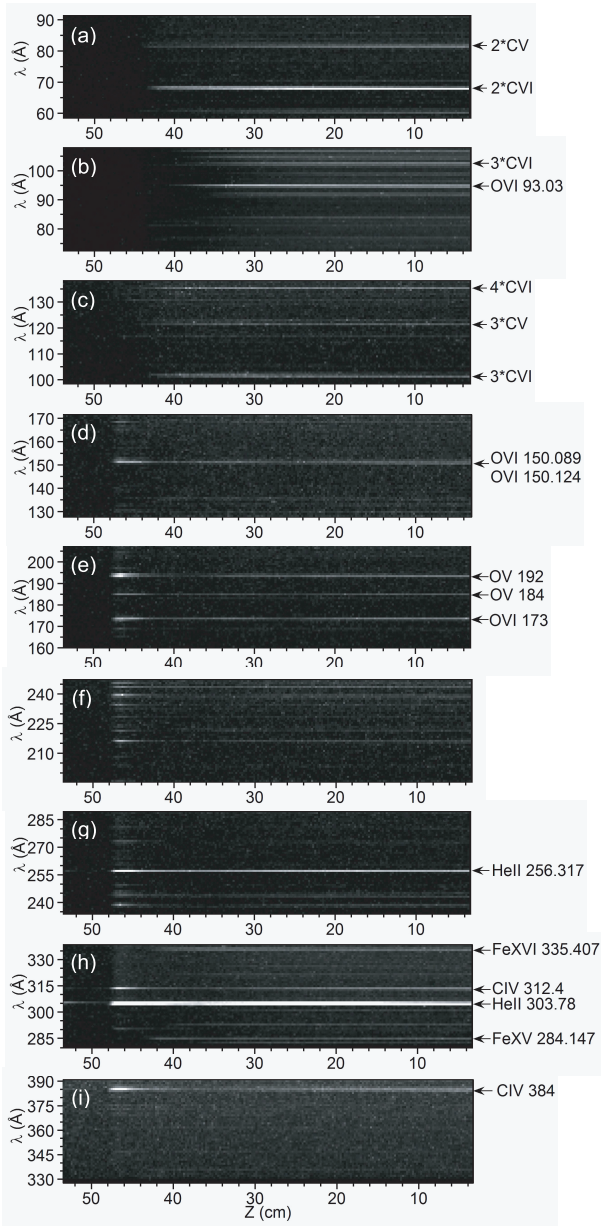


Fig. 1 Two-dimensional CCD images obtained from typical hydrogen LHD discharges. Figures of (a) to (i) show EUV spectral lines in different wavelength regions.

$n_e$ of $7 \times 10^{13}$ cm$^{-3}$ and $T_e(0)$ of 1.3 keV in magnetic axis position of $R_{ax}$ = 3.90 m. It is understood from the figures that only a few EUV lines are emitted with strong intensity at each wavelength range in the normal LHD hydrogen discharges. Impurities are mainly represented by a few elements of helium, carbon and oxygen in the whole EUV range from 60 to 400 Å. Therefore, most of the spectral lines are clearly separated from neighboring lines without blending with other lines. Here, it is noticed that the plasma conditions are not exactly identical during the exposure of nine images in Fig. 1 and Figs. 1 (a) and (b) are obtained at earlier timing of discharges to indicate CV emission clearly.

Two-dimensional CCD images from neon seeded discharges are presented in Figs. 2 (a)-(d) in wavelength range

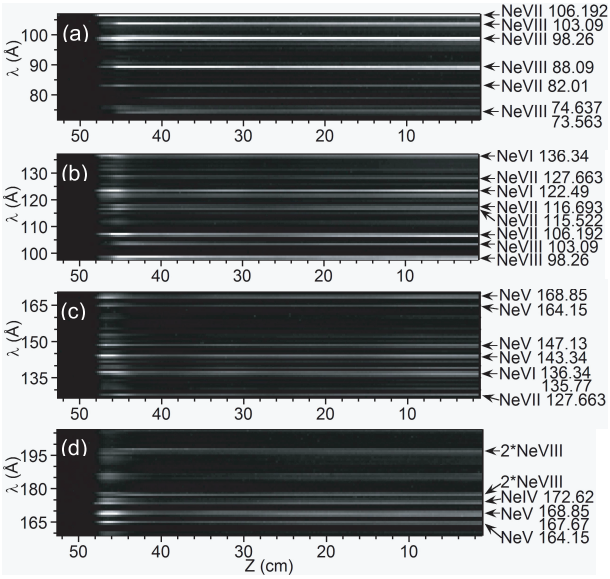


Fig. 2 Two-dimensional CCD images obtained from neon seeded discharges. Figures of (a) to (d) show EUV spectral lines in different wavelength regions.

of 70-210 Å which is a main part showing the neon spectra. The images of the neon spectra greatly differ from ones in the typical hydrogen plasmas seen in Fig. 1. The spectra are fully occupied by the neon ions in various charge states. The intensity of the neon spectral lines is so strong that other spectral lines can not be identified unless the intensity scale is largely expanded. Most of the neon line emissions, however, can be isolated each other indicating an enough space between adjacent two lines.

## 3.2 Radial profiles of spectral lines

Radial profiles of EUV line emissions from several elements in different charge states are illustrated in Figs. 3 (a)-(d). Radial profiles of Figs. 3 (a) and (b) are taken from similar discharges with $T_e(0) = 0.75$ keV at $R_{ax} = 3.60$ m. Since the ionization energies, $E_i$, of HeII ($E_i = 54.4$ eV) and CIV ($E_i = 65$ eV) are quite low those ions are located in the ergodic layer outside the last closed flux surface. The sharp peak in the radial profile seen near $\rho = 1.1$ means line-integrated effect along the same magnetic surface. It is clearly seen that the peak positions of carbon ions are moved inside the plasma according to the charge states. Although the vertical profiles of CV and CVI are the second order, the intensity is still higher than CIV. The CVI is the strongest line among all the charge states of carbon in the EUV range. Spectral lines of HeII, CV and CVI are always used as wavelength markers in calibrating the wavelength in the spectrum.

The radial profiles of NeV to NeVIII in Fig. 3 (c) are taken from similar discharges with $T_e(0) = 3$ keV at $R_{ax} = 3.60$ m. The radial locations of the neon ions are very close each other inside the ergodic layer because the ionization energies of them are not so different, i.e., $E_i = 126$ eV for NeV and $E_i = 239$ eV for NeVIII. Radial

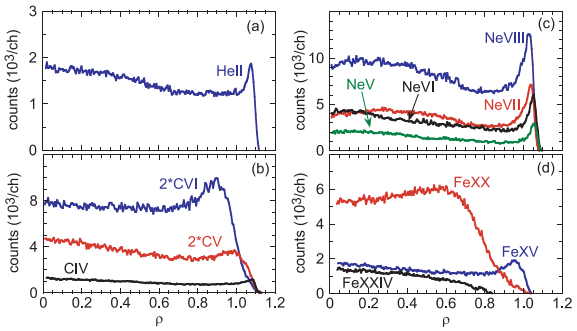


Fig. 3 Radial profiles of EUV spectral lines from different elements; (a) helium: HeII (303.78 Å), (b) carbon: CIV (312.4 Å), CV (2×40.268 Å), CVI (2×33.74 Å), (c) neon: NeV (143.34 Å), NeVI (122.49 Å), NeVII (106.192 Å), NeVIII (98.26 Å) and (d) iron: FeXV (284.15 Å), FeXX (132.85 Å), FeXXIV (192 Å).

profiles of FeXV, FeXX and FeXXIV taken from similar discharges with $T_e(0) = 2.5$ keV at $R_{ax} = 3.60$ m are plotted in Fig. 3 (d). In case of the iron ions, on the other hand, the EUV line emissions are widely distributed over the whole radial location. The highest charge state of iron seen in the EUV range is lithium-like FeXXIV, although helium-like FeXXV can be also observed in LHD at x-ray range of 1.8 Å. The radial profiles of iron ions are obviously different among the ionization stages. The FeXX and FeXXIV are located in the plasma core of $\rho = 0.6$ and $\rho = 0$, respectively, whereas the FeXV is located at plasma edge of near $\rho = 1$. The difference can be simply explained with their different ionization energies (FeXIV: $E_i = 457$ eV, FeXX: $E_i = 1582$ eV and FeXXIV: $E_i = 2.046$ keV). It is noted that the intensity of FeXXIV is considerably smaller than that of FeXX because of the relatively low central temperature of discharges selected for the present study.

## 3.3 Wavelength distribution of EUV spectra

Figures 4 (a)-(d) illustrate the wavelength distribution of EUV spectral lines observed from different discharge conditions, i.e., (a) typical hydrogen discharge, (b) neon seeded discharge, (c) argon seeded discharge and (d) iron pellet injected discharge. It is clearly seen that the number of observed spectral line emissions from the typical hydrogen discharge is quite less and the spectrum is dominated by carbon line emissions of CIV, CV, CVI and HeII as mentioned above. The helium is brought by helium glow discharge cleaning which is being carried out during the night after the end of the experiment in a day.

On the other hand, many strong line emissions are observed in the EUV range for neon, argon and iron. The neon EUV spectral lines mainly exist in wavelength range of 60-210 Å. These strong neon line emissions dominate the EUV spectrum by replacing the carbon line emissions. The neon spectrum mainly consists of charge states from NeIV to NeVIII including extremely strong lines of two lithium-like NeVIII ($1s^2 2s$-$1s^2 3p$: 88.09 Å and $1s^2 2p$-$1s^2 3d$: 98.26 Å) and beryllium-like NeVII (2s2p-2s3p:

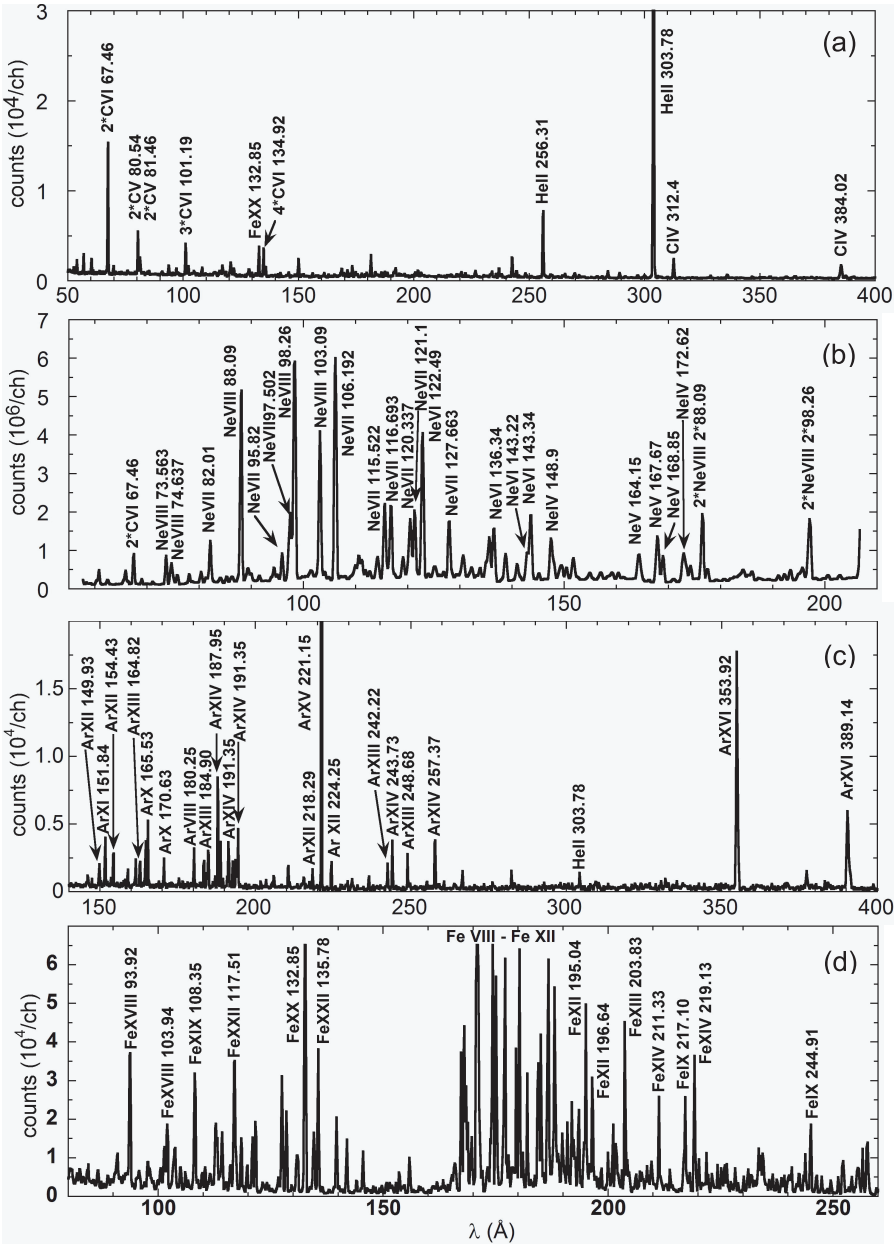


Fig. 4 Wavelength distribution of line emissions from different discharge conditions; (a) typical hydrogen plasmas, (b) neon seeded plasmas, (c) argon seeded plasmas and (d) iron pellet injected plasmas.

106.192 Å). The argon line emissions shown in Fig. 4 (c) mainly exist in wavelength range of 140 to 250 Å. The spectrum covers charge states from ArVIII to ArXVI corresponding to ionization energies from $E_i$ = 143 eV to 918 eV, respectively. The dominant line emissions from argon are beryllium-like ArXV ($1s^2 2s^2$-$1s^2 2s2p$: 221.15 Å) and lithium-like ArXVI ($1s^2 2s$-$1s^2 2p$: 353.92 Å) as well as the neon case. The iron spectrum is presented in Fig. 4 (d) in wavelength range of 80 to 260 Å A variety of charge states of FeVIII to FeXXII is observed in the spectrum having different ionization energies from $E_i$ = 151 eV to 1800 eV, respectively. Many spectral lines from lower ionized iron ions of FeVIII to FeXII are also observed in range of 165 to 195 Å as an emission band. The strongest iron line of FeXX ($2s^2 2s^3$-$2s2p^4$: 132.85 Å) can be clearly seen as an isolated line and other relatively weak lines such as FeXXII and FeXVIII can be also identified. This excellent identification demonstrates an enough spectral resolution in the present spectrometer.

## 4. EUV Bremsstrahlung Continuum

The absolute sensitivity calibration of the EUV spectrometer is very important to calculate absolute intensity of impurity lines. However, there is no standard light source applicable to such a short wavelength region. In order to overcome this problem, a new method using the bremsstrahlung continuum radiation has been developed using LHD high-density plasmas. Recently, a good result is successfully obtained for the EUV_long spectrom-

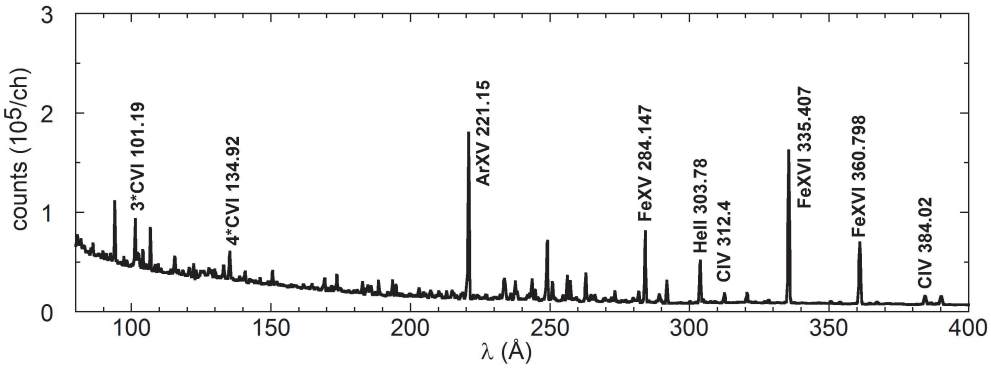


Fig. 5 Wavelength distribution of EUV spectrum including line emissions and bremsstrahlung continuum obtained from hydrogen pellet injected plasmas.

eter [3]. As already known, it is easy to measure the visible bremsstrahlung continuum radiation in fusion plasmas and the absolute sensitivity calibration of the visible spectrometer system can be accurately done using a standard tungsten lamp. Therefore, we try to apply this method to the space-resolved EUV spectrometer system. The bremsstrahlung continuum is enhanced in high-density discharges, in particular, when hydrogen pellets are injected in LHD plasmas. Figure 5 shows the wavelength distribution of EUV spectrum in wavelength range of 80-400 Å including line emissions and bremsstrahlung continuum radiation. The spectrum is obtained from high-density plasmas ($n_e \sim 3.0 \times 10^{14}$ cm$^{-3}$) with hydrogen pellets at $R_{ax}$ = 3.75 m. The bremsstrahlung continuum is clearly observed as background emission of the line spectra. The intensity of the bremsstrahlung continuum increases when the wavelength decreases, suggesting a typical character of the bremsstrahlung continuum.

The certain wavelength interval without line emissions can be easily found from the spectrum in Fig. 5. Figure 6 shows radial profiles of the EUV bremsstrahlung continuum as a parameter of wavelength, i.e., 80 Å, 130 Å, 200 Å and 300 Å. The radial profiles of pure bremsstrahlung continuum radiation are obtained in the EUV range, although the intensity quickly decreases with increase in wavelength. Here, the available wavelength intervals are firstly given in this paper. In order to perform correctly the absolute sensitivity calibration over the whole wavelength range of the present space-resolved spectrometer system, the bremsstrahlung continuum has to be exposed from high-density hydrogen discharges to avoid the interference from line emissions. The hydrogen pellet injection can further improve the accuracy of the sensitivity calibration by enhancing the bremsstrahlung continuum.

The wavelength intervals available for the bremsstrahlung continuum measurement are listed in Table 1 with several line emissions which are also important as the wavelength marker. In the table, 'A' denotes the wavelength intervals in which no other emission lines are included, and 'B' denotes ones in which some line emissions appear in a few discharge conditions. For

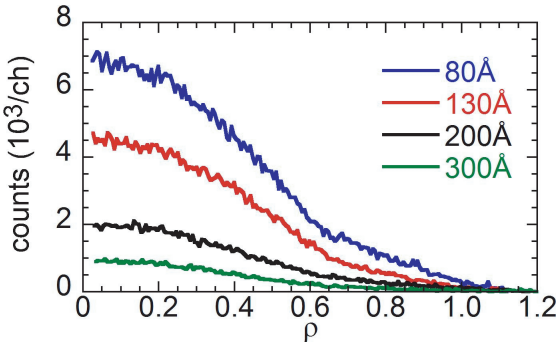


Fig. 6 Radial profiles of EUV bremsstrahlung continuum as a parameter of wavelength.

example, the wavelength interval denoted with B may include line emissions from oxygen at the beginning of experimental campaign and from carbon at extremely high carbon concentration. The absolute calibration of the space-resolved EUV spectrometer can be completed by adopting the wavelength intervals of the bremsstrahlung continuum listed in the Table 1.

## 5. Summary

Radial profiles of spectral line emissions have been measured in wavelength of 60-400 Å using the space-resolved EUV spectrometer with high spectral and spatial resolutions. Vertical profiles of the EUV spectral lines shown with two-dimensional CCD images indicate that the EUV spectrum is dominated by CVI in the typical hydrogen plasma except for HeII and is dominated by NeVII and NeVIII in the neon seeded discharge. Most of the emissions from light impurities are located inside the ergodic layer except for CV and CVI which are located in radial region of $0.8 < \rho < 1$. On the other hand, the line emissions from heavy impurities such as iron widely distribute in the plasma from the plasma edge to the plasma core according to their charge states.

A new method based on the bremsstrahlung continuum radiation to calibrate the EUV spectrometer is studied using high-density discharges of LHD. Strong EUV continuum spectrum is observed with the radial profile from

Table 1 Wavelength intervals of EUV bremsstrahlung continuum available for absolute calibration of EUV spectrometer. Impurity line emissions indicated are useful for wavelength calibration.

| Wavelength (Å) | Spectrum | Remark |
|---|---|---|
| 82-93 | bremsstrahlung continuum | A |
| 94.5-100 | bremsstrahlung continuum | A |
| 101.19 | 3×CVI 1s-2p | |
| 102-132 | bremsstrahlung continuum | B |
| 132.85 | FeXX $2s^22p^3$-$2s2p^4$ | |
| 134.92 | 4×CVI 1s-2p | |
| 136-149 | bremsstrahlung continuum | A |
| 152-181 | bremsstrahlung continuum | B |
| 182.097 | CVI 2s-3p | |
| 182.23 | CVI 2s-3d | |
| 183.4-191 | bremsstrahlung continuum | B |
| 192.8 | OV 2s2p-2s3d | |
| 194-220 | bremsstrahlung continuum | A |
| 221.15 | ArXV $1s^22s^2$-$1s^22s2p$ | |
| 222-248 | bremsstrahlung continuum | B |
| 258-283 | bremsstrahlung continuum | B |
| 284.147 | FeXV $3s^2$-3s3p | |
| 285-291 | bremsstrahlung continuum | A |
| 292.5-302 | bremsstrahlung continuum | A |
| 303.78 | HeII 1s-2p | |
| 305-311 | bremsstrahlung continuum | A |
| 312.4 | CIV $1s^22s$-$1s^23p$ | |
| 313-334 | bremsstrahlung continuum | B |
| 335.407 | FeXVI $2p^63s$-$2p^63p$ | |
| 337-359 | bremsstrahlung continuum | A |
| 360.798 | FeXVI $2p^63s$-$2p^63p$ | |
| 362-383 | bremsstrahlung continuum | A |
| 384.02 | CIV $1s^22p$-$1s^23s$ | |
| 385-400 | bremsstrahlung continuum | B |

hydrogen pellet injected high-density discharges using the space-resolved EUV spectrometer. The wavelength intervals of the EUV bremsstrahlung continuum available for the absolute calibration of the present system are listed with remarks. The bremsstrahlung profiles presented in this paper are also important to measure the $Z_{\rm eff}$ profile in the EUV range.

# Acknowledgments

This work was partially carried out under the LHD project financial support (NIFS10ULPP010) and also partially supported by the JSPS-CAS Core-University program in the field of 'Plasma and Nuclear Fusion.'

[1] D. Robinson *et al*., Appl. Opt. **6**, 40 (1967).
[2] M. B. Chowdhuri, S. Morita and M. Goto, Appl. Opt. **47**, 135 (2008).
[3] M. B. Chowdhuri, S. Morita, M. Goto, H. Nishimura, K. Nagai and S. Fujioka, Rev. Sci. Instrum. **78**, 023501 (2007).
[4] J. K. Lepson *et al*., J. Phys. B: At. Mol. Opt. Phys. **43**, 144018 (2010).
[5] C. Dong, S. Morita, M. Goto and H. Zhou, Rev. Sci. Instrum. **81**, 033107 (2010).
[6] E. S. Marmar *et al*., Rev. Sci. Instrum. **46**, 1149 (1975).
[7] H. Nozato, S. Morita, M. Goto *et al*., Rev. Sci. Instrum. **74**, 2032 (2003).
[8] TFR Group and J. F. Wyart, Physica Scripta **37**, 66 (1988).
[9] C. Breton *et al*., Physica Scripta **37**, 33 (1988).
[10] M. B. Chowdhuri, S. Morita, M. Goto *et al*., Plasma Fusion Res. **2**, S1060 (2007).
[11] M. J. May *et al*., Nucl. Fusion **37**, 881 (1997).
[12] M. Finkenthal *et al*., J. Phys. B: At. Mol. Phy. **18**, 4393 (1985).
[13] U. Feldman *et al*., Astron Astrophys. **441**, 1211 (2005).